1822–1829 Nucleic Acids Research, 1995, Vol. 23, No. 10

Multiple protein–DNA interactions over the yeast *HSC82* heat shock gene promoter

Alexander M. Erkine, Christopher C. Adams+, Mingxing Gao and David S. Gross*

Department of Biochemistry and Molecular Biology, Louisiana State University Medical Center, PO Box 33932, Shreveport, LA 71130, USA

Received November 22, 1994; Revised and Accepted March 30, 1995

ABSTRACT

We have utilized DNase I and micrococcal nuclease (MNase) to map the chromatin structure of the *HSC82* heat shock gene of *Saccharomyces cerevisiae*. The gene is expressed at a high basal level which is enhanced 2–3-fold by thermal stress. A single, heat-shock invariant DNase I hypersensitive domain is found within the *HSC82* chromosomal locus; it maps to the gene's 5′ end and spans 250 bp of promoter sequence. DNase I genomic footprinting reveals that within this hypersensitive region are four constitutive protein–DNA interactions. These map to the transcription initiation site, the TATA box, the promoter-distal heat shock element (HSE1) and a consensus GRF2 (REB1/Factor Y) sequence. However, two other potential regulatory sites, the promoter-proximal heat shock element (HSE0) and a consensus upstream repressor sequence (URS1), are not detectably occupied under either transcriptional state. In contrast to its sensitivity to DNase I, the nucleosome-free promoter region is relatively protected from MNase; the enzyme excises a stable nucleoprotein fragment of ~210 bp. As detected by MNase, there are at least two sequence-positioned nucleosomes arrayed 5′ of the promoter; regularly spaced nucleosomes exhibiting an average repeat length of 160–170 bp span several kilobases of both upstream and downstream regions. Similarly, the body of the gene, which exhibits heightened sensitivity to DNase I, displays a nucleosomal organization under both basal and induced states, but these nucleosomes are not detectably positioned with respect to the underlying DNA sequence and may be irregularly spaced and/or structurally altered. We present a model of the chromatin structure of *HSC82* and compare it to one previously derived for the closely related, but differentially regulated, *HSP82* heat shock gene.

INTRODUCTION

DNA within the nucleus of a eukaryotic cell is complexed with histones and a variety of non-histone chromosomal proteins to form chromatin. The primary subunit of chromatin is the nucleosome, whose core consists of 165 bp of DNA coiled around a histone octamer, and whose linker is of variable length, ranging from 0 to 80 bp (1). Since the initial observation that actively transcribed sequences are preferentially susceptible to digestion by DNase I (2,3), nuclease digestion has been widely used to study the relationship between chromatin structure and gene expression.

The yeast *Saccharomyces cerevisiae* provides an ideal system for dissecting the relationship between gene structure and function (4). To date, the detailed chromatin structure of a variety of yeast genes has been described, including the mating-type loci (5), the two alcohol dehydrogenase genes (6), the galactose-regulated *GAL* genes (7–10), *PHO5* (11), *LEU2* (12) and the heat shock gene *HSP82* (13). These studies have revealed that actively transcribed yeast genes, like those in higher eukaryotes, typically possess promoter-associated nuclease hypersensitive sites and transcription units with heightened sensitivity to DNase I (reviewed in 14,15). While hypersensitive sites are thought to represent nucleosome-free entry points for regulatory proteins, displacement or disruption of nucleosomes may arise from the direct binding of regulatory proteins to nucleosomal DNA (16–20; reviewed in 21,22). Alternatively, histone binding to DNA may be pre-empted by the selective deposition of transcription factors onto chromatin during nucleosome assembly (23). The general increase in nuclease sensitivity of transcription units is thought to be due to traversing RNA polymerase molecules that transiently disrupt or displace nucleosomes, possibly through the generation of positive supercoils (24–26) or through direct competition of the polymerase for the DNA (10,27). In addition, long arrays of phased nucleosomes are frequently observed in regions flanking transcribed sequences, but their functional significance, if any, remains unclear (13,28–30).

We are interested in understanding the role of chromatin in the heat shock transcription mechanism, and are employing the closely related *HSP82* and *HSC82* genes of *S.cerevisiae* as biological models. As a prelude to a detailed genetic and biochemical dissection of this mechanism, it is necessary to obtain a high-resolution map of the chromatin structure of these differentially regulated genes. The nucleoprotein architecture of the strongly inducible *HSP82* gene has been previously described, and includes structures potentially involved in transcription initiation, elongation and

* To whom correspondence should be addressed

+Present address: Department of Biochemistry and Molecular Biology, 301 Althouse Laboratory, The Pennsylvania State University, University Park, PA 16802, USA

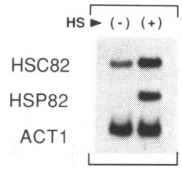

Figure 1. Steady-state *HSP90* mRNA levels in yeast cells before and after heat shock. Total RNA was prepared from log-phase cells either maintained at 30°C (–) or heat-shocked for 15 min (+), and subjected to Northern analysis as described in Materials and Methods.

termination (4,13,31). We have performed a complementary study on the *HSC82* gene, which is expressed at a 10-fold higher constitutive level but is induced only 2–3-fold following heat shock, based on both protein and RNA measurements (32; Fig. 1). We report here that the chromatin structure of the *HSC82* locus reflects its constitutively high level of transcription, and in many ways resembles that elucidated for *HSP82*. However, in contrast to *HSP82*, we find that the nucleosome-free promoter region of *HSC82* is remarkably resistant to micrococcal nuclease (MNase) and contains, by the criteria of DNase I genomic footprinting, four prominent protein–DNA interactions. These interactions map to the transcription initiation (Inr) site, the TATA box, the promoter-distal heat shock element (HSE1) and a consensus GRF2 (REB1/Factor Y) site. The latter complex is not seen within the *HSP82* promoter (20,31,33), and may underlie the MNase resistance of the *HSC82* upstream region.

MATERIALS AND METHODS

Cell growth, heat shock and spheroplasting

S.cerevisiae haploid strain W303-1B [MATα, *ade2-1*, *can1*-100, *his3*-11,15, *leu2*-3,112, *trp1*-1, *ura3*-1 (ref. 20)] was used in all experiments reported here. Cells were grown in rich medium (1% yeast extract, 2% bacto-peptone, 2% dextrose) to early log phase (~2.5×10^7 cells/ml), heat shocked (30–39°C shift for 15–20 min), metabolically poisoned with 20 mM sodium azide and converted to spheroplasts at 30°C as previously described (31).

Nuclease digestion of chromatin

For micrococcal nuclease digestions, nuclei were purified from a 250 ml mid-log culture (~3.5×10^7 cells/ml) as described by Szent-Gyorgyi *et al.* (13) and gently suspended in 600 µl of digestion buffer [10 mM HEPES (pH 7.5), 0.5 mM $MgCl_2$, 0.05 mM $CaCl_2$) fortified with the following battery of protease inhibitors: 1 mM PMSF, 2.0 mM benzamidine, 0.1 µg chymostatin/ml, 1.7 µg aprotinin/ml, 1.1 µg phosphoramidon/ml, 7.2 µg E-64/ml, 1.0 µg pepstatin/ml, 2.0 µg leupeptin/ml, 2.0 µg antipain/ml. Suspended nuclei were divided into 200 µl samples (~50 µg DNA), prewarmed at 37°C for 5 min, and digested with MNase (Pharmacia) employing 800 U/sample for 10 min or 400 U/sample for 20 min.

For DNase I digestions, spheroplast lysates rather than purified nuclei were employed as the substrate. We have previously found that the lysate technique gives equal or superior DNase I chromatin and genomic footprints (31). Spheroplasts, lysed in 40 mM Hepes, pH 7.2, 1 mM $MgCl_2$, 0.1 mM $CaCl_2$ (supplemented with the same complement of protease inhibitors as above), were digested with DNase I (DPFR grade; Organon Teknika, Malvern, PA) using 4 Kunitz U/sample [each sample representing the equivalent of ~5×10^9 cells (~60 µg DNA)] for 10 min at 23°C or 3–14 U/sample for 80 min at 3°C, and genomic DNA was purified as described (31).

For digestion of naked DNA as a control, DNA was purified from nuclei as above and digested at 37°C for 10 min with 2×10^{-5} U DNase I/µg DNA or 2×10^{-2} U MNase/µg DNA. Nuclease cleavage sites were mapped by electrophoresing the foregoing samples in parallel with molecular weight standards (*Hin*dIII digested λ DNA + *Hae*III digested ϕX174 DNA) and/or with landmark restriction fragments (see legends to Figs 3, 6 and 7). Landmark fragments were obtained by digesting genomic DNA with *Bam*HI alone (–1341, +4100) or with one of the following enzymes: *Hae*III (–714), *Eco*RI (–615), *Hin*dIII (–370, +2095), *Xba*I (–173, –285) or *Kpn*I (+553). Nucleotide coordinates are provided relative to the principal transcription start site, located 41 bp upstream of the ATG codon (32).

DNA electrophoresis and Southern blot hybridization

DNA samples (7.5 µg/lane) were electrophoresed on a 2% agarose gel in 40 mM Tris, 33 mM sodium acetate, 2 mM EDTA (pH 8.5) and blotted by alkaline capillary transfer to nylon (34). MNase and DNase I cleavage sites were mapped by indirect end-labelling (35,36). DNA was restricted with *Bam*HI prior to electrophoresis and hybridized with probes **C1** and **C4** to permit mapping from the upstream and downstream anchors, respectively (see Fig. 2A for probe and restriction map). All blots were hybridized and washed at 55°C with RNA probes synthesized *in vitro* using pGEM-3 (**C1**, **C3**, **C4**) or pRS306 (**C2**) constructs as previously described (37). *HSC82*-specific fragments were subcloned out of pUTX203 (a gift of D. B. Finkelstein), a pBR322 derivative containing the 4.5 kb *HSC82* *Bam*HI fragment (spanning –1341 to +4100).

Genomic primer extension of DNase I digested chromatin

Spheroplast lysates were prepared essentially as above except that spheroplasting was done at 30°C for control cells and 39°C for heat-shocked cells. Lysates were digested with 0–80 U of DNase I per 5×10^9 cells at 23°C for 5 min. Reactions were terminated through addition of an equal volume of stop buffer (50 mM Tris–HCl, pH 7.5, 1 M NaCl, 1% SDS and 50 mM EDTA). Following incubation at 23°C for 15 min, cellular debris was pelleted (14 000 *g*, 1 min), the supernatant extracted with phenol–chloroform, and nucleic acids precipitated with an equal volume of isopropanol. Nucleic acids were then suspended in 10 mM Tris–HCl, 0.5 mM EDTA, pH 8.0 (TE buffer), sequentially digested with RNase A and proteinase K, phenol–chloroform extracted and ethanol precipitated. Each sample was then suspended in 100 µl TE, chromatographed through a Sephadex G50 spin column, ethanol precipitated, and dissolved in 50 µl distilled water. Deproteinized genomic DNA control samples were digested with 0–0.2 U DNase I per 5 µg DNA at 23°C for 5 min, ethanol precipitated, and dissolved in 20 µl distilled water. The overall level of digestion of chromatin and naked DNA was assessed by agarose gel electrophoresis; samples were matched according to extent of digestion. Only samples exhibiting low to intermediate levels of digestion were subjected to primer extension, optimizing the probability of there being no more than one cleavage within the *HSC82* upstream regulatory region (38).

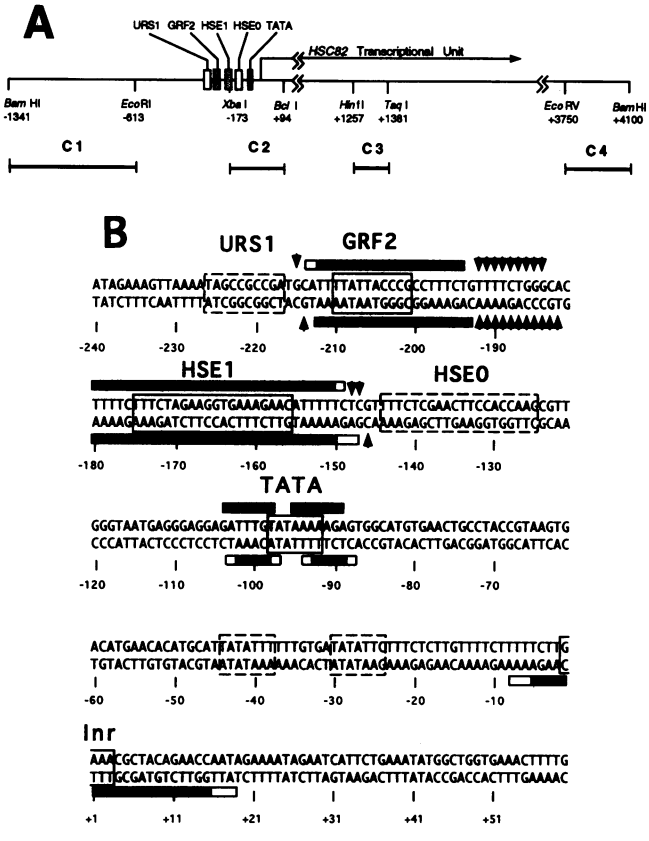

Figure 2. Physical map of the *HSC82* locus, DNA sequence of the promoter region, and summary of DNase I genomic footprinting analysis. (**A**) Strategy for mapping the chromatin structure of the *HSC82* heat shock locus. The indicated restriction fragments (**C1–C4**) were isolated from pUTX203 and subcloned into pGEM-3 for use as templates in *in vitro* transcription reactions catalyzed by either SP6 (**C1**) or T7 (**C2–C4**) RNA polymerase. Filled rectangles represent regulatory sites shown in this study to be constitutively occupied in chromatin; the open rectangles depict sites that remain vacant. The arrow spans a region of ~2.3 kb. (**B**) The *HSC82* upstream sequence is numbered relative to the principal transcription start site (+1), as defined by S1 mapping (32). Putative *cis*-regulatory sequences within the *HSC82* upstream regulatory region, identified by their similarity to published consensus sequences (51), are indicated. In addition, the four continuously boxed elements, GRF2, HSE1, TATA and Inr, serve as binding sites for sequence-specific proteins based both on DNase I genomic footprinting of spheroplast lysates (this paper) and a mutational analysis to be published elsewhere (Adams *et al.*, manuscript in preparation). The GRF2 element centered at position –205 exhibits an 8/8 match to conserved nucleotides within its consensus sequence, YNNYYACCCG (where Y = C or T) (59), while TATA boxes at –98, –41 and –27 exhibit 7/7, 6/7 and 5/7 matches, respectively, to the TATA consensus, TATAWAW (where W = A or T) (43,44). Heat shock elements HSE0 and HSE1 each exhibit a 10/12 match to conserved nucleotides within the heat shock consensus, consisting of four tandemly inverted NTTCN units (55). The URS1 sequence centered at position –221 exhibits a 10/10 match to the URS consensus, TAGCCGCCGA (61), whereas the Inr element centered at +1 exhibits a 3/4 match to the consensus, YAWR (where R = A or G) (63). The extent of strand-specific protection from DNase I is indicated by solid bars drawn where discernable cutting exists in naked DNA; where no cleavage is present in the naked DNA, open bars have been drawn to indicate uncertainty in the limit of the footprint. Arrowheads indicate nucleotides hypersensitive to cleavage by DNase I. Nucleotide protections and hyperreactivities are unchanged following heat shock. Note that the upper strand has not been mapped downstream of position –50, while the lower strand has not been mapped upstream of position –230 (see Figs 4 and 5).

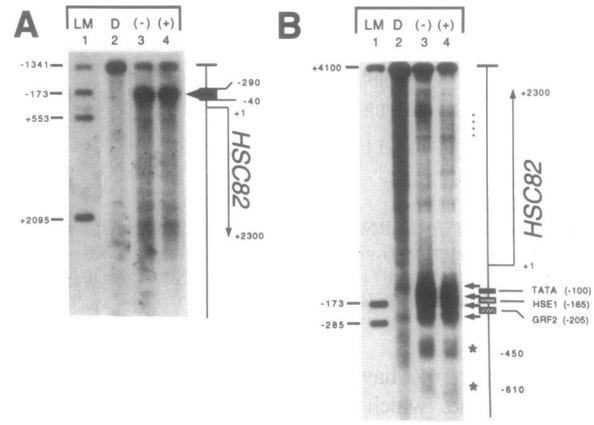

Figure 3. DNase I chromatin footprints of the *HSC82* locus ± heat shock. (**A**) Yeast spheroplast lysates, derived from non-heat shocked (–) and 15 min heat shocked (+) cells, were digested with DNase I as described in Materials and Methods (lanes 3 and 4). Deproteinized DNA (D) was similarly digested (lane 2). The DNA was purified and subjected to indirect end-labelling with probe **C4**. The hypersensitive site mapping to the 5′ end of *HSC82* is indicated by the bold arrow; the region corresponding to the transcription unit is also indicated. Cleavage sites were mapped using landmark fragments (LM; lane 1) whose upstream end-points are indicated on left. (**B**) Same as (A), except *HSC82*-specific cleavage profiles were illuminated with probe **C1**. Bold arrows indicate the location of four strong cut sites within the DNase I hypersensitive domain; these map to positions –75, –135, –200 and –270. Asterisks (*) indicate the location of weaker chromatin-specific cleavage sites. A shorter autoradiographic exposure of lane 2 verifies that the 3′ sites, like those at the 5′ end, are chromatin-specific (data not shown).

One microgram of genomic DNA was subjected to amplified primer extension (AMPEX) essentially as described (39). Briefly, 10 pmol of oligonucleotide was end-labelled with 100 μCi γ-ATP and gel purified; this provided sufficent primer for 20 AMPEX reactions (0.5–1.0 × 10^6 c.p.m./reaction). These reactions employed sequencing-grade *Taq* DNA polymerase (Promega) and the following parameters: denaturation, 94°C for 2 min; annealing, 65°C for 20 min; and extension, 72°C for 1 min. The reaction products were precipitated with 2 vol of ethanol, electrophoresed on an 8% sequencing gel (1:30 acrylamide:bisacrylamide), and the *HSC82*-specific DNase I cleavage profile revealed by PhosphorImager (Molecular Dynamics) analysis using ImageQuant software. The *HSC82*-specific oligonucleotides employed in this study were: 5′-CTATTTTCTATTGGTTCTCTGTAGCG-3′ (spanning nucleotides +25 to +2 of the lower strand) and 5′-CTTTCTTTTTGTATTCATAGAACAGC-3′ (spanning nucleotides –277 to –252 of the upper strand).

RNA electrophoresis and Northern blot hybridization

RNA samples were prepared from control and 15 min heat shocked cells, electrophoresed, blotted and UV-crosslinked to GeneScreen, and hybridized to gene-specific probes as described (37). *HSC82* mRNA was detected using antisense RNA probe **C3** (see Fig. 2A), *HSP82* mRNA was detected using a synthetic oligonucleotide homologous to its 3′ end [spanning positions +2226 to +2287 (20)], and *ACT1* mRNA was detected using a 1.6 kb antisense RNA probe homologous to its coding region. Stringent hybridization conditions were employed (65°C hybridization and wash for **C3**, 45°C hybridization and wash for *HSP82*) that resulted in minimal or no (*HSP82*) detectable cross-hybridization between the closely related *HSP90* transcripts.

RESULTS

A single DNase I hypersensitive site is found within the *HSC82* locus and maps to the gene's promoter region

To map the chromatin structure of *HSC82*, we digested spheroplast lysates obtained from control and heat-shocked cells with DNase I. The resultant DNA was purified, restricted with *Bam*HI, and, following electrophoresis and blotting, indirectly end-labelled with probe **C4** (see Fig. 2A for probe map). As shown in Figure 3A, such a procedure reveals the presence of a single DNase I hypersensitive site, marking the 5′ end of the gene and seen irrespective of heat shock. It is notable that other than the *HSC82* promoter region, there are no sequences hypersensitive to DNase I within the 5.5 kb locus. Also evident from this experiment is the presence of a single broad region of heightened DNase I sensitivity mapping to the *HSC82* transcriptional unit. Taken together, these data suggest that *HSC82* is the only active gene within this locus under these experimental conditions (see Discussion).

To obtain a complementary map of *HSC82* chromatin structure, we hybridized a blot containing similar DNA samples with **C1**, which abuts the upstream *Bam*HI site. As illustrated in Figure 3B, such an approach confirms the presence of a constitutive DNase I hypersensitive region extending ~40–280 bp upstream of the gene. Within this hypersensitive domain are several internal regions that appear to be protected from DNase I cleavage and are unchanged by heat shock; these are mapped at nucleotide precision below. Extending upstream from the DNase I hypersensitive domain are alternating regions of protection and cleavage spaced at ~160 bp intervals. These accessible sites (large asterisks) may indicate the presence of nucleosomal linkers (see below). Downstream, the DNase I cutting pattern is largely indistinguishable from that of the naked DNA control. However, four chromatin-specific bands, mapping to the 3′ end of the *HSC82* coding region and spaced at ~150 bp intervals, can be seen [Fig. 3B, lanes 3 and 4 (small asterisks)]. While these may correspond to the linker regions of tandemly positioned nucleosomes, such nucleosomes appear to be altered in some fashion since they are not recognized by micrococcal nuclease (see Fig. 7 below).

Genomic primer extension reveals constitutive DNase I protection at both upstream and downstream *HSC82* promoter elements

To characterize protein–DNA interactions over the *HSC82* upstream region more precisely, we mapped cleavage sites at nucleotide resolution using genomic primer extension analysis. Briefly, spheroplast lysates were generated as above, digested with DNase I, and genomic DNA was purified and subjected to primer extension with a radiolabelled oligonucleotide specific for either upper or lower strand (see Materials and Methods). Strand-specific interactions were discerned by comparing the cleavage pattern of DNA in chromatin with the pattern observed for naked genomic DNA.

Four regions of protection are revealed by such an analysis. Most prominent is a strong footprint centered over the promoter-distal heat shock element, termed HSE1. The HSE1 footprint spans ~30 bp, from –180 to –150, and is evident on each strand (Figs 4 and 5). Augmented sensitivity is seen at the periphery of the footprint, particularly upstream. Both the breadth of the footprint and flanking hyperreactivity are highly characteristic of heat shock factor (HSF)–heat shock element (HSE) interactions (31,40). Occupancy of HSE1 is unaltered by heat shock (data not shown), consistent with the notion that yeast HSF binds to DNA constitutively (31,41,42). A second region of constitutive protection maps to the consensus GRF2 site located 20 bp upstream of HSE1. The DNase I protection at this sequence, which spans –212 to –193, appears to be stronger on the upper strand (compare Figs 4 and 5, lanes 8 and 9; note that the same DNA samples were employed in generating the two footprints). Whether this is unique to the GRF2 interaction at *HSC82* or is a general property of its binding to DNA *in vivo* is unknown; preferential interaction with the C-rich strand of *ENO1* was not seen *in vitro* (60). It is noteworthy that neither the consensus upstream repressor sequence (URS1) nor the promoter-proximal heat shock element, HSE0, is detectably occupied under either transcriptional state (see Discussion).

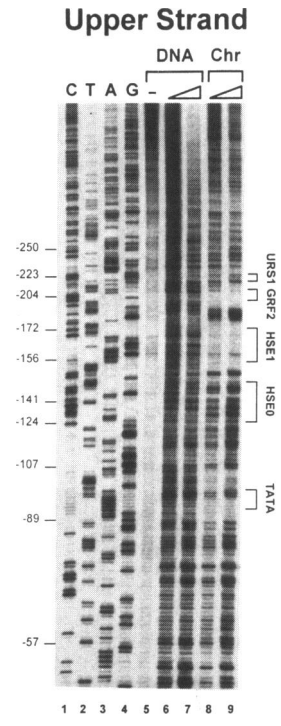

Figure 4. DNase I upper strand genomic footprint of the *HSC82* promoter region. Lanes 1–4, sequencing ladders generated by amplified primer extension using genomic DNA as the template and an oligonucleotide complementary to the *HSC82* upper strand (spanning positions +25 to +2) as the primer. Lane designations refer to upper strand sequence. Lanes 5–7, naked genomic DNA digested with 0, 0.01 or 0.04 U DNase I/μg DNA at 23°C for 5 min. Lanes 8 and 9, spheroplast lysates derived from non-heat-shocked cells were digested with increasing amounts of DNase I, genomic DNA purified, and subjected to amplified primer extension using the +25 oligonucleotide as above (see Materials and Methods). Locations of potential regulatory elements are provided on right, nucleotide coordinates numbered with respect to the transcription start site are provided on left.

Within the core promoter region, two sites of strong protection are seen. Most prominent is the TATA-binding protein (TBP)–TATA interaction between positions –104 and –89. Interestingly, there is an internal segment corresponding to the first 2–3 bp of the core TATAAA motif that is highly accessible to DNase I [particularly evident on the upper strand (Fig. 4, lanes 8 and 9)]. This pattern of protection and accessibility is retained following heat shock (data not shown). The accessibility of this internal region may result from the severe helical distortion and sharp kinking of DNA which are known to accompany binding of TBP to TATA (43,44). We have detected

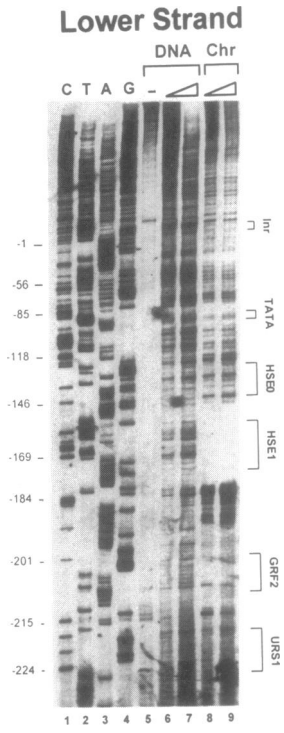

Figure 5. DNase I lower strand genomic footprint of the *HSC82* promoter region. Genomic primer extension was performed with an *HSC82*-specific nucleotide complementary to the lower strand and spanning positions –277 to –252. Samples and labelling of lanes are the same as in Figure 4.

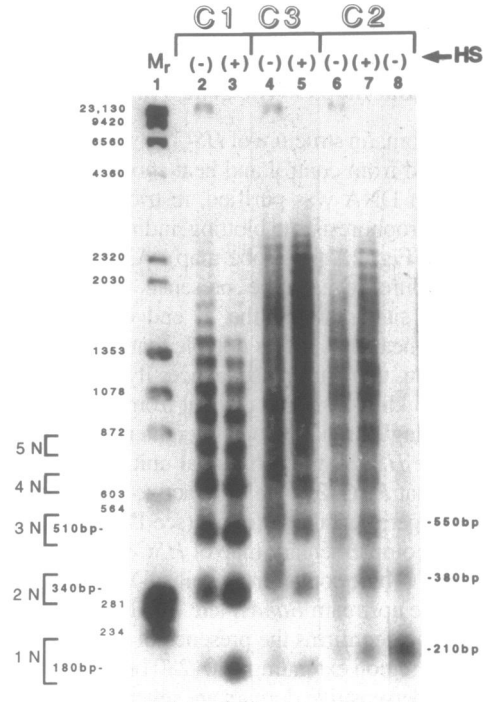

Figure 6. MNase-generated nucleosomal ladders detected using upstream-, coding region- and promoter-specific probes. Nuclei, purified from control (–) and 15 min heat-shocked (+) cells, were digested with MNase as described in Materials and Methods. DNA was purified, electrophoresed through 2% agarose gels, transferred to Zeta-Probe and hybridized to *HSC82*-specific probes **C1**, **C2** and **C3** as indicated. Sizing of DNA fragments was done using co-electrophoresed end-labelled molecular weight standards (lane 1; see Materials and Methods). Identical DNA samples were employed in the MNase ladders of lanes 2, 4 and 6 and 3, 5 and 7; the **C1**- and **C2**-generated patterns are derived from sequential hybridizations of the same blot and are precisely aligned. The **C2**-illuminated pattern in lane 8 represents a more extensively digested non-heat-shocked sample. MNase digestion of naked genomic DNA yielded a random cleavage pattern in each region of the *HSC82* locus examined (data not shown). **1N–5N** correspond to integral multiples of the nucleosome repeat (160–170 bp). Sizes of monomer-, dimer- and trimer-length DNA fragments detected by the **C1** and **C2** hybridization probes are provided on left and right, respectively.

a similar region of internal hypersensitivity within the TATA element of the *HSP82* gene (31,33). Partial DNase I protection can also be discerned in the region downstream of the consensus TATA box (Fig. 5 and data not shown). While this region contains two alternative TATA elements (Fig. 2B), this protection may signify the presence of an extended open polymerase complex, such as previously described at *GAL1* and *GAL10* (64). This possibility is strengthened by the presence of a second region of strong protection within the core promoter, spanning the transcription initiation site (positions –5 to +15) and seen irrespective of heat shock (Fig. 5 and data not shown). A summary of the genomic footprinting data is presented in Figure 2B.

The upstream region is organized into regularly spaced nucleosomes while the promoter is packaged into a non-nucleosomal, MNase-resistant particle

The DNase I indirect end-labelling experiments suggest that DNA sequences upstream of the *HSC82* promoter region are packaged in a relatively DNase I-resistant state, those downstream of the promoter are in a state of heightened accessibility, while those within the promoter are hypersensitive to DNase I cleavage. To more clearly assess the extent to which nucleosomes occupy these regions, we digested nuclei isolated from control and heat-shocked cells with micrococcal nuclease, an enzyme that preferentially hydrolyzes the DNA linking adjacent nucleosomes. Genomic DNA was electrophoresed, blotted, and sequentially hybridized with probes spanning the *HSC82* locus. Within the distal upstream region, MNase generates well-resolved nucleosomal ladders exhibiting a repeat length of ~170 bp [Fig. 6, lanes 2 and 3 (probe **C1**)], similar to that of *S.cerevisiae* bulk chromatin (45,46). Under optimal conditions, ladders with 20 discrete bands have been observed. A similar result has been obtained using the far downstream probe **C4** (data not shown). We conclude that irrespective of the transcriptional state of the gene, the distal 5′ and 3′ flanking regions are packaged into regularly spaced, canonical nucleosomes.

Using the coding region probe (**C3**), a ladder-like pattern of DNA fragments is also detected (Fig. 6, lanes 4 and 5). The predominant nucleosomal repeat length within the coding region appears similar to that of the flanking regions (~165 bp). However, as indicated by the high interband background, there is a strong tendency for MNase to cleave at intervals other than 165 bp. This suggests that a subpopulation of nucleosomes are irregularly spaced and/or disrupted within the *HSC82* transcriptional unit. Such disruption may underlie the DNase I sensitivity of the coding region (Fig. 3), and resembles that previously seen within the *HSP82* transcriptional unit (25). It is notable that despite the presence of altered structures within the coding region, relatively sharp bands are seen in the higher oligomers ($\geq$ 12 N) detected by **C3**. Thus it appears that spacing characteris-

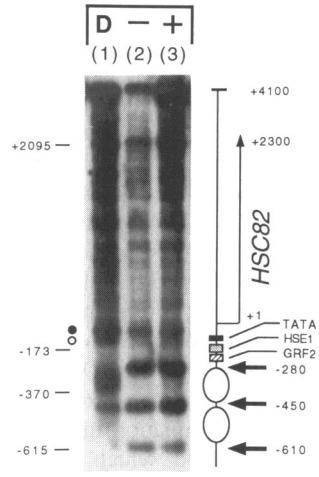

Figure 7. MNase chromatin footprint of the *HSC82* chromatin locus ± heat shock. Nuclei, purified from control (–) and 15 min heat-shocked (+) cells, were digested with MNase as described in Materials and Methods. Deproteinized DNA (D) was similarly digested. DNA was then purified and subjected to indirect end-labelling with probe **C1**; cleavage sites were mapped using landmark fragments whose mobilities are indicated on left. Chromatin-specific cleavages are indicated by bold arrows; these correspond to the linker regions of positioned nucleosomes (ovals). The approximate locations of regulatory sites within the promoter are indicated (rectangles), as is the location of the *HSC82* transcriptional unit (thin arrow). The open circle indicates the position of a strong cut site in DNA protected in chromatin (mapping to –110); the filled circle indicates the position of a site strongly cut in both DNA and chromatin (mapping to –60). Locations of protections and accessible sites are based on measurements from two independent experiments.

tic of nucleosomes is maintained throughout the transcriptional unit, resulting in a single register of nucleosomes throughout the 5.5 kb mapped region.

Since the *HSC82* promoter region was hypersensitive to digestion with DNase I, we anticipated that MNase would cleave the promoter into subnucleosomal-length fragments as previously observed for the *HSP82* promoter (20). Unexpectedly, however, we found that the promoter-specific probe (**C2**) detected a stable product larger than a nucleosome (~210 bp); this fragment was resistant to even extensive digestion (Fig. 6, lane 8). The increased resistance of the promoter to MNase is also indicated by its slower digestion kinetics compared to those seen in the 5′ intergenic region within the same DNA samples (lanes 6 and 7 versus lanes 2 and 3). This result indicates that the sequence-specific factors identified above, along with perhaps other DNA binding proteins (such as histones), mimic a nucleosome in their ability to protect the promoter sequences from internal MNase cleavage. Measurement of the fragment lengths of the dimer, trimer, and higher oligomers reveals spacing at 160–170 bp intervals, consistent with the nucleosome repeat length of the surrounding regions.

Sequence-positioned nucleosomes extend upstream from the DNase I hypersensitive promoter

To determine whether the nucleosomes in the upstream region were positioned with respect to the underlying DNA sequence, we mapped MNase cleavage sites using indirect end-labelling as above. As revealed in Figure 7, three prominent cleavages spaced at 160–170 bp intervals are seen in the chromatin samples ± heat shock. These bands are either specific to chromatin (position –280) or are much more intensely cut in chromatin than in naked DNA (positions –450 and –610; compare lanes 2 and 3 with lane 1). The spacing and intensity of these cleavages suggests the presence of two sequence-positioned nucleosomes, an interpretation supported by the strong interband protections centered at –370 and –530. Also consistent with this view are broad DNase I cleavages that map to the putative linker regions (Fig. 3B, large asterisks). A third prominent MNase cut site is seen at position –780 in other experiments (data not shown), suggesting the presence of a tandem array composed of at least three nucleosomes. However, as the latter cleavage maps within the region of the probe used for indirect end-labelling (**C1**, spanning –1341 to –613), its location must be considered tentative.

Several other interesting features of the *HSC82* locus are revealed by this analysis. The promoter region, in stark contrast to its hypersensitivity to DNase I, is relatively resistant to MNase. The resistant domain spans ~210 bp and is flanked by two strong cut sites at –280 and –60 (Fig. 7, arrow and filled circle, respectively), fully consistent with the nucleosomal ladder analysis discussed above. Notably, a strong cleavage site in naked DNA mapping to the TATA region is protected in nuclei ± heat shock (Fig. 7, open circle). Thus, MNase and DNase I appear to recognize complementary structural features of the promoter; in particular, MNase cuts only at the periphery of the region hypersensitive to DNase I. No chromatin-specific MNase cleavages or protections are evident within the transcriptional unit or 3′ flanking region (Fig. 7 and data not shown).

DISCUSSION

In the present study, we have dissected the chromatin structure of the constitutively transcribed *HSC82* gene. We have found that despite a nearly complete divergence of upstream nucleotide sequence (Fig. 8A), the structural organization of *HSC82* bears a strong resemblance to that previously described for its inducible counterpart, *HSP82* (4,13,31) (nucleoprotein structures summarized in Fig. 8B). In both genes, a broad DNase I hypersensitive domain marks the 5′ end of the gene, overlapping the promoter region. This hypersensitivity is constitutive, and resembles that seen at the 5′ ends of other heat shock genes in yeast (47), *Drosophila* (36,48,49) and mammals (50). Within these hypersensitive domains are internal footprints reflecting the presence of sequence-specific regulatory proteins. While the transcription units of each gene exhibit a nucleosomal character, these nucleosomes are altered or disrupted, as evidenced by the high interband background in the MNase ladder analysis and the increased sensitivity of the coding region to DNase I. Moreover, each gene is flanked on the 5′ and 3′ ends with nucleosomes, a number of which are sequence-positioned. Notably, the basic architecture of each gene remains unchanged following heat shock.

Close examination of the structural data reveal a number of interesting differences as well. First, within the mapped region of the *HSC82* locus, there is a single DNase I hypersensitive site, while there are five such sites within a comparable region of the *HSP82* locus (4,13,25,52). As nuclease hypersensitive sites mark the location of crucial *cis*-regulatory sequences (14,15), their abundance at *HSP82* may reflect the greater complexity of its upstream region as well as the presence of several closely packed genes. Indeed, the hypersensitive cluster centered at –615 may potentially function in the regulation of *HSP82* and/or a divergently oriented upstream gene (51). Moreover, immediately

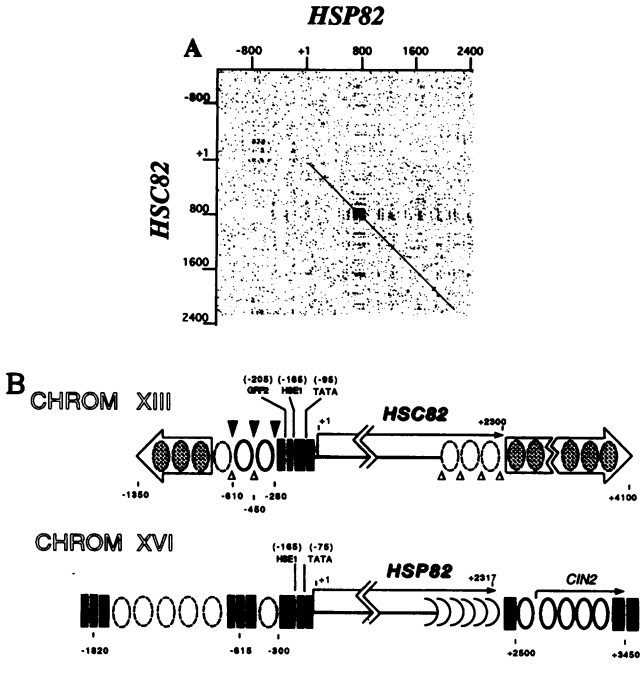

Figure 8. DNA sequence organization and chromatin structure of the yeast *HSP90* genes. (**A**) Dot matrix comparison of gene sequences (where +1 signifies the transcription start site). The analysis employed a stringency of 60% and a window of 10 bp (Geneworks 2.3). A comparative analysis of regulatory sequence motifs is presented elsewhere (51). (**B**) Models of *HSC82* and *HSP82* chromatin structure, as deduced from nuclease digestion experiments described here and elsewhere (4,13,25,31,52). Neither locus shows detectable structural alteration following heat shock. DNase I hypersensitive sites are depicted as solid bars; internal footprints are represented as gaps. Nucleosomes whose positioning has been established are indicated by continuous ovals; those whose positioning is less firmly established are indicated by broken ovals. Regions of regularly spaced nucleosomes are depicted by filled ovals; the boxes signify that the positions of the nucleosomes within these regions have not been mapped. Structures cleaved by DNase I at half-nucleosomal intervals are represented by semi-ovals. The 5′ ends of the *HSP82*, *HSC82* and *CIN2* transcripts, as well as the 3′ end of the *HSP82* transcript, have been mapped (25,32,62). The 3′ coordinates of *HSC82* and *CIN2* are based on electrophoretic mobility of their transcripts (2.3 and 0.9 kb, respectively) and are therefore only approximate. The location of chromatin-specific, non-hypersensitive MNase and DNase I cleavages mapped at the *HSC82* locus in this study are shown as filled and open triangles, respectively. Adapted from Szent-Gyorgyi *et al.* (13).

downstream of *HSP82* is the *CIN2* gene; its transcription start site is only 182 bp beyond the 3′ end of *HSP82* and a hypersensitive site marks its promoter region (25; see Fig. 8B). A similar analysis of the *HSC82* upstream region failed to detect the presence of transcripts homologous to either strand (data not shown). Therefore, the absence of DNase I hypersensitive sites within the *HSC82* locus, save the one associated with its promoter, suggests that under these experimental conditions, *HSC82* is the only active gene within the 5.5 kb locus.

A second difference in chromatin structure between the two genes is the MNase sensitivity of their respective promoter regions. Strong cut sites bookend a relatively resistant region within the *HSC82* promoter, resulting in the generation of a stable 210 bp fragment and mimicking a mononucleosome. In contrast, other than a partial protection over the TATA box, MNase cuts the upstream region of *HSP82* in a manner indistinguishable from that of naked DNA (13). Most significantly, it degrades the *HSP82* promoter region into submonomer-length fragments under conditions in which the 210 bp fragment derived from the *HSC82* promoter remains stable (Fig. 6 and ref. 20). The intrinsic resistance of the *HSC82* promoter to micrococcal nuclease resembles that previously reported for the *GAL1–GAL10* intergenic regulatory region. This nucleosome-free region, site of four UAS_G elements and a GRF2 binding site, is processed by MNase to a stable fragment of 90–130 bp (9), large enough to accommodate the 108 bp encompassing these sequences (53). It is interesting that *HSC82*, in contrast to *HSP82* but like *GAL1–GAL10*, bears a consensus GFR2 site within its upstream region (see below).

A third area of difference between the two genes is in the fine structure of their 3′ ends. In *HSP82*, a DNase I cutting interval of ~80 bp is observed in this region, and extends at least 480 bp from the site of transcription termination into the body of the gene (13,25). This cleavage period, which is thought to reflect the presence of 'split' or half nucleosomes, is strictly dependent on transcription (25). *HSC82* likewise exhibits a chromatin-specific DNase I cleavage pattern at its 3′ terminus (Fig. 3B). However, these cleavages occur with nucleosomal (~150 bp) rather than half-nucleosomal periodicity. The significance of this difference is unclear, particularly since *HSC82* is strongly transcribed irrespective of heat shock, based on both Northern analysis (Fig. 1) and β-galactosidase assays of *HSC82–lacZ* gene fusions (Adams and Gross, unpublished observations). Split nucleosomes are thought to result from waves of positive supercoiling generated ahead of traversing RNA polymerase II molecules (25,26; reviewed in ref. 54). Therefore, it is possible that such torsion is more effectively dissipated at *HSC82* than at the 3′ end of *HSP82*, where a topological anchorage site is presumed to exist between the heat shock gene and *CIN2* (25).

The fourth and perhaps most interesting difference pertains to the pattern of protection within the promoter-associated DNase I hypersensitive domain. Four genomic footprints, corresponding to sequence-specific protein–DNA interactions, are found within the *HSC82* upstream region. In each promoter, two regulatory elements, the TATA box and a heat shock element located ~170 bp upstream of the transcription start site (termed HSE1 in each case), are protected (Figs 4 and 5; refs 20,31,33). In addition, two other sites, a consensus GRF2 sequence and the principal transcription start site, are protected within the *HSC82* promoter. That HSE1, TATA and GRF2 elements are functional *in vivo* has been confirmed by mutational analysis of each promoter (20,33,52; Adams *et al.*, in preparation; S. F. Simmons and D. S. Gross, unpublished results).

It is interesting that in each promoter multiple sequences bearing homology to the eukaryotic heat shock consensus sequence (HSCS) exist, yet in each promoter only one element is stably bound by protein, presumably heat shock factor (HSF). In *HSC82*, the promoter-proximal heat shock element, HSE0, is vacant under both transcriptional states despite exhibiting a 10/12 match to conserved nucleotides of the HSCS [considered here as four tandem inverted repeats of NTTCN (55)]. This vacancy, which has been confirmed by dimethyl sulfate *in vivo* footprinting (data not shown), is all the more surprising since HSE0 exhibits the same degree of homology to the HSCS as does the constitutively footprinted sequence, HSE1. Nonetheless, *in situ* mutagenesis confirms that HSE0 plays little if any detectable role in regulating *HSC82* transcription (Adams *et al.*, in preparation). Similarly, within the *HSP82* promoter, two elements exhibit 9/12 matches to the HSCS, one centered at –167 (HSE1) and the other

centered at −198 (HSE2), yet only the former is constitutively occupied by protein as revealed by DNase I, DMS and hydroxyl radical genomic footprinting experiments (20,31,33). Thus, the promoter-distal HSE appears to be the most critical for promoter function in *HSC82*, whereas the promoter-proximal HSE is the critical UAS in *HSP82*. These results are consistent with suggestions that additional nucleotides besides the conserved TTC/GAA core sequences are important in heat shock element function (56,57). Indeed, within each HSE1 is the octameric sequence TTCTAGAA, a motif unique to these elements within their respective promoters and characteristic of most, if not all, heat shock genes in *S.cerevisiae* (58).

Finally, our DNase I genomic footprinting experiments reveal the presence of constitutive protection over the GRF2 site located upstream of HSE1. GRF2 is an abundant yeast nuclear protein; binding sites for GRF2 are found within numerous UAS regions, as well as within centromeres, telomeres and the 35S ribosomal RNA enhancer (59). It has been previously shown that GRF2 binding to DNA results in a local 230 bp nucleosome-free region within chromatin; deletion of the GRF2 site within the *GAL1–GAL10* intergenic region leads to nucleosome encroachment over the mutated sequence (28). While exhibiting weak transcriptional activation on its own, GRF2 can function synergistically with other elements (59). What might be its function upstream of *HSC82*? We have previously shown that the HSF–HSE1 complex plays a critical role in creating the nucleosome-free region upstream of *HSP82*; recent mutagenesis experiments suggest a similarly important role for the HSE1 sequence upstream of *HSC82* (Adams *et al.*, in preparation). GRF2 may also contribute to the nucleosome-free state of the *HSC82* promoter, particularly given its proximity to the HSF–HSE1 complex. Moreover, as discussed above, its presence may underlie the MNase protection seen within this region. We are currently testing these possibilities.

ACKNOWLEDGEMENTS

We thank Bill Garrard and Chris Szent-Gyorgyi for thoughtful comments on an earlier version of this manuscript and David Finkelstein for generously providing us with plasmid pUTX203. This work was supported by grants from the National Institute of General Medical Sciences (GM45842) and the Center for Excellence in Cancer Research at LSUMC awarded to DSG.

REFERENCES

1 van Holde, K.E. (1989) *Chromatin*, Springer, New York.
2 Weintraub, H. and Groudine, M. (1976) *Science* **193**, 848–856.
3 Garel, A. and Axel, R. (1976) *Proc. Natl. Acad. Sci. USA* **73**, 3966–3970.
4 Gross, D.S., Szent-Gyorgyi, C., and Garrard, W.T. (1986) *UCLA Symp. Mol. Cell.Biol. New Ser.* **33**, 345–366.
5 Nasmyth, K.A. (1982) *Cell* **30**, 567–578.
6 Sledlewski, A. and Young, E.T. (1982) *Proc. Natl. Acad. Sci. USA* **79**, 253–256.
7 Lohr, D. (1983) *Nucleic Acids Res.* **11**, 6755–6773.
8 Lohr, D. (1993) *Proc. Natl. Acad. Sci. USA* **90**, 10628–10632.
9 Fedor, M.J. and Kornberg, R.D. (1989) *Mol. Cell. Biol.* **9**, 1721–1732.
10 Cavalli, G. and Thoma, F. (1993) *EMBO J.* **12**, 4603–4613.
11 Almer, A., Rudolph, H., Hinnen, A., and Horz, W. (1986) *EMBO J.* **5**, 2689–2696.
12 Martinez-Garcia, J.F., Estruch, F., and Perez-Ortin, J.E. (1989) *Mol. Gen. Genet.* **217**, 464–470.**217**, 464–470.
13 Szent-Gyorgyi, C., Finkelstein, D.B., and Garrard, W.T. (1987) *J. Mol. Biol.* **193**, 71–80.**193**, 71–80.
14 Elgin, S.C.R. (1988) *J. Biol. Chem.* **263**, 19259–19262.
15 Gross, D.S. and Garrard, W.T. (1988) *Ann. Rev. Biochem.* **57**, 159–197.
16 Fascher, K.-D., Schmitz, J., and Horz, W. (1990) *EMBO J.* **9**, 2523–2528.
17 Pina, B., Bruggemeier, U., and Beato, M. (1990) *Cell* **60**, 719–731.
18 Archer, T.K., Cordingley, M.G., Wolford, R.G., and Hager, G.L. (1991) *Mol. Cell. Biol.* **11**, 688–698.**11**, 688–698.
19 Morse, R.H. (1993) *Science* **262**, 1563–1566.
20 Gross, D.S., Adams, C.C., Lee, S., and Stentz, B. (1993) *EMBO J.* **12**, 3931–3945.
21 Workman, J.L. and Buchman, A.R. (1993) *Trends Biochem. Sci.* **18**, 90–95.
22 Wolffe, A.P. (1994) *Cell* 77, 13–16.
23 Svaren, J. and Chalkley, R. (1990) *Trends Genet.* **6**, 52–56.
24 Lui, L.F. and Wang, J.C. (1987) *Proc. Natl. Acad. Sci. USA* **84**, 7024–7027.
25 Lee, M.-S. and Garrard, W.T. (1991) *EMBO J.* **10**, 607–615.
26 Lee, M.-S. and Garrard, W.T. (1991) *Proc. Natl. Acad. Sci. USA* **88**, 9675–9679.
27 van Holde, K.E., Lohr, D.E. and Robert, C. (1992) *J. Biol. Chem.* **267**, 2837–2840.
28 Fedor, M.J., Lue, N.F., and Kornberg, R.D. (1988) *J. Mol. Biol.* **204**, 109–127.
29 Thoma, F. and Simpson, R.T. (1985) *Nature* **315**, 250–252.
30 Kornberg, R.D. and Stryer, L. (1988) *Nucleic Acids Res.* **16**, 6677–6690.
31 Gross, D.S., English, K.E., Collins, K.W., and Lee, S. (1990) *J. Mol. Biol.* **216**, 611–631.
32 Borkovich, K.A., Farrelly, F.W., Finkelstein, D.B., Taulien, J., and Lindquist, S. (1989) *Mol. Cell. Biol.* **9**, 3919–3930.
33 McDaniel, D., Caplan, A.J., Lee, M.-S., Adams, C.C., Fishel, B.R., Gross, D.S., and Garrard, W.T. (1989) *Mol. Cell. Biol.* **9**, 4789–4798.
34 Reed, K.C. and Mann, D.A. (1985) *Nucleic Acids Res.* **13**, 7207–7221.
35 Nedospasov, S.A. and Georgiev, G.P. (1980) *Biochem. Biophys. Res. Commun.* **92**, 532–539.
36 Wu, C. (1980) *Nature* **286**, 854–860.
37 Adams, C.C. and Gross, D.S. (1991) *J. Bacteriol.* **173**, 7429–7435.
38 Galas, D.J. and Schmitz, A. (1978) *Nucleic Acids Res.* **5**, 3157–3170.
39 Huibregtse, J.M. and Engelke, D.R. (1991) *Methods Enzymol.* **194**, 550–562.
40 Wiederrecht, G., Shuey, D.J., Kibbe, W.A., and Parker, C.S. (1987) *Cell* **48**, 507–515.
41 Sorger, P.K., Lewis, M.J., and Pelham, H.R.B. (1987) *Nature* **329**, 81–84.
42 Jakobsen, B.K. and Pelham, H.R.B. (1988) *Mol. Cell. Biol.* **8**, 5040–5042.
43 Kim, Y., Geiger, J.H., Hahn, S., Sigler, P.B. (1993) *Nature* **365**, 512–520.
44 Kim, J.L., Nikolov, D.M., and Burley, S.K. (1993) *Nature* **365**, 520–527.
45 Lohr, D., Kovacic, R.T., and van Holde, K.E. (1977) *Biochemistry* **16**, 463–471.
46 Szent-Gyorgyi, C. and Isenberg, I. (1983) *Nucleic Acids Res.* **11**, 3717–3736.
47 Pederson, D.S. and Morse, R.H. (1990) *EMBO J.* **9**, 1873–1881.
48 Cartwright, I.L. and Elgin, S.C.R. (1986) *Mol. Cell. Biol.* **6**, 779–791.
49 Costlow, N.A., Simon, J.A., and Lis, J.T. (1985) *Nature* **313**, 147–149.
50 Brown, M.E., Amin, J., Schiller, P., Voellmy, R., and Scott, W.A. (1988) *J. Mol. Biol.* **203**, 107–117.
51 Erkine, A.M., Szent-Gyorgyi, C., Simmons, S.F., and Gross, D.S. (1995) *Yeast* **11**, in press.
52 Lee, M.-S. and Garrard, W.T. (1992) *Proc. Natl. Acad. Sci. USA* **89**, 9166–9170.
53 Johnston, M. and Davis, R.W. (1984) *Mol. Cell. Biol.* **4**, 1440–1448.
54 Thoma, F. (1991) *Trends Genet.* **7**, 175–177.
55 Xiao, H. and Lis, J.T. (1988) *Science* **239**, 1139–1142.
56 Amin, J., Ananthan, J., and Voellmy, R. (1988) *Mol. Cell. Biol.* **8**, 3761–3769.
57 Fernandes, M., Xiao, H., and Lis, J.T. (1994) *Nucleic Acids Res.* **22**, 167–173.
58 Tuite, M.F., Bossier, P., and Fitch, I.T. (1988) *Nucleic Acids Res.* **16**, 11845.
59 Chasman, D.I., Lue, N.F., Buchman, A.R., LaPointe, J.W., Lorch, Y. and Kornberg, R.D. (1990) *Genes Dev.* **4**, 503–514.
60 Carmen, A.A. and Holland, M.J. (1994) *J. Biol. Chem.* **269**, 9790–9797.
61 Luche, R.M., Sumadra, R. and Cooper, T.G. (1990) *Mol. Cell. Biol.* **10**, 3884–3895.
62 Farrelly, F.W. and Finkelstein, D.B. (1984) *J. Biol. Chem.* **259**, 5745–5751.
63 Furter-Graves, E.M. and Hall, B.D. (1990) *Mol. Gen. Genet.* **223**, 407–416.
64 Giardina, C. and Lis, J.T. (1993) *Science* **261**, 759–762.